The Journal of Physiology

Sensorimotor integration within the primary motor cortex by selective nerve fascicle stimulation

Federico Ranieri[1], Giovanni Pellegrino[2], Anna Lisa Ciancio[3], Gabriella Musumeci[4,5], Emiliano Noce[3], Angelo Insola[4], Lorenzo Alirio Diaz Balzani[6], Vincenzo Di Lazzaro[4] and Giovanni Di Pino[5]

[1] *Unit of Neurology, Department of Neuroscience Biomedicine and Movement Sciences, University of Verona, Verona, Italy*
[2] *Department of Neurology and Neurosurgery, Montreal Neurological Institute, McGill University, Montreal, Quebec, Canada*
[3] *Research Unit of Biomedical Robotics and Biomicrosystems, Campus Bio-Medico University, Rome, Italy*
[4] *Unit of Neurology Neurophysiology and Neurobiology, Department of Medicine, Campus Bio-Medico University, Rome, Italy*
[5] *Research Unit of Neurophysiology and Neuroengineering of Human-Technology Interaction (NeXTlab), Campus Bio-Medico University, Rome, Italy*
[6] *Unit of Orthopaedics and Traumatology, Department of Medicine, Campus Bio-Medico University, Rome, Italy*

Edited by: Richard Carson & Vaughan Macefield

Linked articles: This article is highlighted in a Perspectives article by Oddo. To read this article, visit https://doi.org/10.1113/JP282734.

The peer review history is available in the Supporting information section of this article (https://doi.org/10.1113/JP282259#support-information-section).

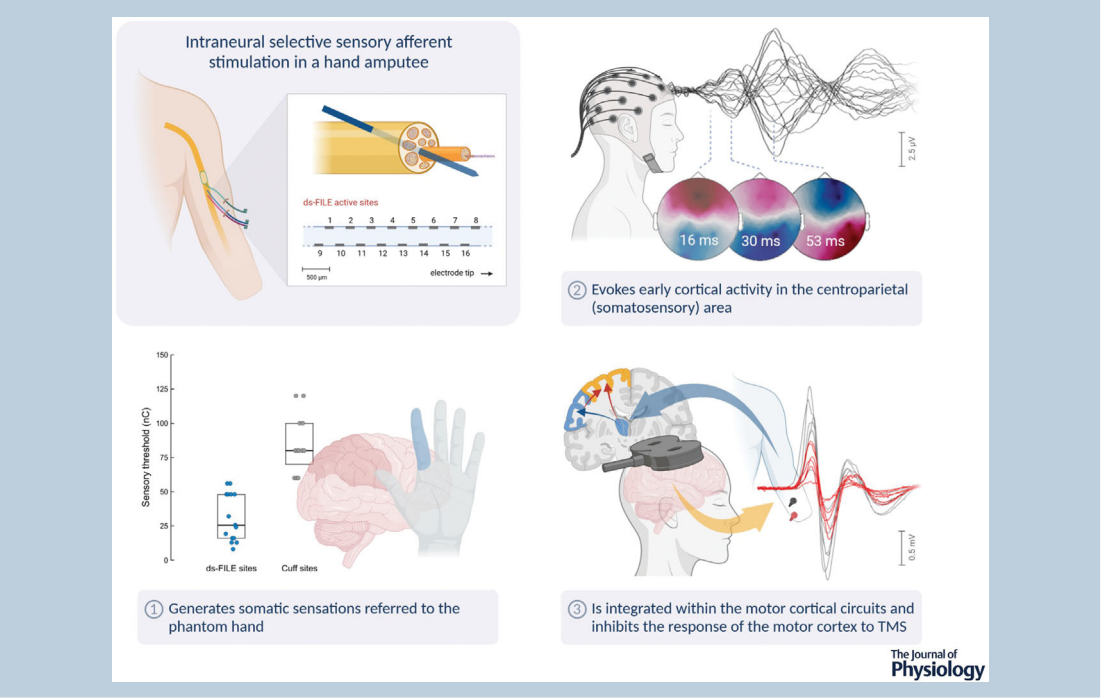

Federico Ranieri is Neurologist and Researcher at the Department of Neuroscience, Biomedicine and Movement Sciences of the University of Verona, Italy. He obtained his Medical Degree and PhD Degree in Neuroscience at the Catholic University of Rome and then he worked as post-doctoral researcher at the Campus Bio-Medico University of Rome, Italy. His main areas of interest are human brain plasticity, and the physiology and pathophysiology of the sensorimotor system, investigated by means of non-invasive brain stimulation methods. He also contributed to the understanding of the physiological bases of non-invasive brain stimulation.

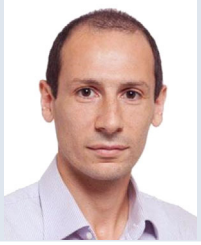

DOI: 10.1113/JP282259

Abstract The integration of sensory inputs in the motor cortex is crucial for dexterous movement. We recently demonstrated that a closed-loop control based on the feedback provided through intraneural multichannel electrodes implanted in the median and ulnar nerves of a participant with upper limb amputation improved manipulation skills and increased prosthesis embodiment. Here we assessed, in the same participant, whether and how selective intraneural sensory stimulation also elicits a measurable cortical activation and affects sensorimotor cortical circuits. After estimating the activation of the primary somatosensory cortex evoked by intraneural stimulation, sensorimotor integration was investigated by testing the inhibition of primary motor cortex (M1) output to transcranial magnetic stimulation, after both intraneural and perineural stimulation. Selective sensory intraneural stimulation evoked a low-amplitude, 16 ms-latency, parietal response in the same area of the earliest component evoked by whole-nerve stimulation, compatible with fast-conducting afferent fibre activation. For the first time, we show that the same intraneural stimulation was also capable of decreasing M1 output, at the same time range of the short-latency afferent inhibition effect of whole-nerve superficial stimulation. The inhibition generated by the stimulation of channels activating only sensory fibres was stronger than that due to intraneural or perineural stimulation of channels activating mixed fibres. We demonstrate in a human subject that the cortical sensorimotor integration inhibiting M1 output previously described after the experimental whole-nerve stimulation is present also with a more ecological selective sensory fibre stimulation.

(Received 13 August 2021; accepted after revision 13 December 2021; first published online 17 December 2021)
Corresponding authors Federico Ranieri, MD, PhD: Unit of Neurology, Department of Neuroscience, Biomedicine and Movement Sciences, University of Verona, P.le L.A. Scuro 10, 37134 Verona, Italy. Email: federico.ranieri@univr.it
Giovanni Di Pino, MD, PhD: Research Unit of Neurophysiology and Neuroengineering of Human-Technology Interaction (NeXTlab), Campus Bio-Medico University, Via Alvaro del Portillo 21, 00128 Roma, Italy. Email: g.dipino@unicampus.it

Abstract figure legend Double-sided filament electrodes (ds-FILE), bearing 16 active sites, and perineural *Cuff* electrodes were implanted in the median and ulnar nerve of the arm in a hand amputee (upper left panel, single nerve represented). Selectivity of stimulation (1), evoked activity in the somatosensory cortex (2) and sensorimotor integration (3) were investigated. TMS: transcranial magnetic stimulation. [Image created with BioRender.com.]

Key points

- Cortical integration of sensory inputs is crucial for dexterous movement.
- Short-latency somatosensory afferent inhibition of motor cortical output is typically produced by peripheral whole-nerve stimulation.
- We exploited intraneural multichannel electrodes used to provide sensory feedback for prosthesis control to assess whether and how selective intraneural sensory stimulation affects sensorimotor cortical circuits in humans.
- Activation of the primary somatosensory cortex (S1) was explored by recording scalp somatosensory evoked potentials. Sensorimotor integration was tested by measuring the inhibitory effect of the afferent stimulation on the output of the primary motor cortex (M1) generated by transcranial magnetic stimulation.
- We demonstrate in humans that selective intraneural sensory stimulation elicits a measurable activation of S1 and that it inhibits the output of M1 at the same time range of whole-nerve superficial stimulation.

Introduction

Sensory afferent modulation of the output of the motor cortex focuses muscle activation in dexterous and fine movement and is part of sensorimotor integration: the exploitation of multimodal sensory information to produce voluntary goal-directed movements.

In recent years, several studies have investigated how to provide somatic sensory feedback from hand prostheses by means of interfaces with the peripheral nerve

(Dhillon *et al*. 2004; Rossini *et al*. 2010; Ortiz-Catalan *et al*. 2014; Raspopovic *et al*. 2014; Tan *et al*. 2014; Oddo *et al*. 2016; Valle *et al*. 2018; D'Anna *et al*. 2019; Petrini *et al*. 2019; Zollo *et al*. 2019; Mastinu *et al*. 2020).

Encouraging, yet preliminary, results have shown improvement of manipulation skills due to sensory feedback (Raspopovic *et al*. 2014; Valle *et al*. 2018; Zollo *et al*. 2019), and amelioration of amputation-induced maladaptive plasticity (Rossini *et al*. 2010; Di Pino *et al*. 2012, 2020; Ferreri *et al*. 2014). However, intraneural afferent stimulation is not sufficiently mature to produce a physiological perception of touch. Among neural interfaces, intraneural stimulating electrodes allow higher stimulation selectivity compared to perineural electrodes (Navarro *et al*. 2005). For this reason, despite some limitations related to limited long-lasting stability (Lotti *et al*. 2017; Gori *et al*. 2021) and other issues affecting their performance (Ciancio *et al*. 2016; Cutrone & Micera, 2019; Strauss *et al*. 2019), these electrodes may be suitable to provide near-physiological sensations.

Recently, we exploited the potential of intraneural electrodes having active stimulating sites on both faces of the polyimide body (double-sided filament electrodes: ds-FILE) embedded in a closed-loop control algorithm providing an afferent feedback: we demonstrated improved grasping capabilities and slippage control of a myoelectric hand prosthesis (Zollo *et al*. 2019), and increased prosthesis embodiment (Di Pino *et al*. 2020). Of note, the improvement of motor skill associated with the training with afferent feedback was paralleled by a reduction of sensorimotor-driven inhibitory plasticity within the primary motor cortex (M1) (Zollo *et al*. 2019). How the afferent information delivered through intraneural stimulation was integrated with the motor output at the cortical level remained to be defined.

Anatomical, behavioural and physiological studies provide consistent evidence that motor and sensory cortices have a compensatory but equally important role in motor control. Indeed, besides sensory to motor cortex interactions mediated by cortico-cortical and thalamo-cortical connections (Hooks, 2017), and cortico-striatal networks (Robbe, 2018; Dubbioso *et al*. 2019), animal studies have shown the existence of descending projections arising from S1 and higher order somatosensory areas and reaching lower motor stations, which can directly generate movement (Rathelot & Strick, 2006; Matyas *et al*. 2010; Rathelot *et al*. 2017).

The set of experiments presented in this paper, conducted in the hand amputee described in Zollo *et al*. (2019), aims to shed light on the physiological bases of the selective sensory feedback provided by intraneural stimulation, by determining whether it produces a reliable cortical activation and affects sensorimotor cortical circuits (i.e. if it generates sensorimotor integration). The demonstration of a reliable activation of sensorimotor cortical circuits would support the hypothesis that the observed improvement of prosthesis control relates to the activation of specific afferent fibres. Thus, we investigated the cortical activation and the sensorimotor integration after selective peripheral nerve fibre stimulation delivered by both intraneural and perineural electrodes.

Activation of the primary somatosensory cortex (S1) was explored by recording somatosensory evoked potentials (SEPs) using surface scalp electrodes.

Sensorimotor integration was tested by measuring the inhibitory effect of the afferent stimulation on the output of M1 generated by transcranial magnetic stimulation (TMS), namely the short-latency afferent inhibition (SAI) (Tokimura *et al*. 2000). The course of this inhibition is time-locked with the short-latency negative SEP component recorded from parietal regions, and generated by the early activation of S1, probably by multiple cell depolarization (Eisen, 1982; Peterson *et al*. 1995).

When it is induced by superficial stimulation of the whole nerve at the wrist it is commonly recorded with a latency of about 20 ms, and hence it is known as N20. The SAI phenomenon relies on inhibition of corticospinal output mediated by the activation of central cholinergic (Di Lazzaro *et al*. 2000) and possibly GABAergic circuits (Di Lazzaro *et al*. 2007). Functionally, it could be considered as a long loop reflex, the cortical counterpart of the spinal stretch reflex (Bertolasi *et al*. 1998).

By means of the SAI protocol, we tested fast connection pathways of thalamic afferents to M1 corticospinal circuits. For the first time, we observed in humans that selective nerve fascicle stimulation through intraneural electrodes is capable of both depolarizing S1 neurons and producing strong and selective inhibition of M1 output at short inter-stimulus intervals.

Methods

Ethical approval

The study was conducted in accordance with the *Declaration of Helsinki* and following amendments, except for registration in a database, and it was approved by the Ethics Committee of Campus Bio-Medico University (Approval ref.: 15/16 PAR ComEt CBM, 29/03/2016) and by the Italian Ministry of Health (Approval ref.: 0003992-19/01/2017-DGDMF-MDS-P). The participant provided written informed consent.

Participant

Tests were performed on a female subject (age: 40 years) who suffered traumatic amputation at the middle third of the left forearm (forearm stump length: ∼10 cm) at the age of 8 years. The subject was implanted with perineural and

intraneural electrodes in the arm nerves (see below), and she participated in a set of experiments to test the efficacy of invasive peripheral nerve stimulation for the feedback control of a robotic hand prosthesis (Zollo *et al.* 2019).

Experimental design

Motor responses and perceived sensations evoked by perineural and intraneural stimulation of median and ulnar nerves of the arm were preliminarily mapped, to obtain information on the selectivity of both techniques of invasive nerve stimulation.

Cortical activation was then assessed by recording scalp SEPs with a 32-channel EEG system.

Finally, sensorimotor integration was investigated by testing the inhibitory effect of peripheral afferent stimuli on motor cortical excitability, as assessed through the SAI protocol (Tokimura *et al.* 2000). Specifically, we evaluated the changes of the motor evoked potential (MEP) amplitude induced by preconditioning the cortex with afferent stimulation.

Data obtained with invasive stimulation were compared with those of transcutaneous nerve stimulation.

Neural electrodes

Six invasive neural electrodes were implanted through a microsurgery intervention accessing the medial aspect of the middle third of the left arm following the medial edge of the biceps muscle and exposing the ulnar and the medial nerves for about 5 cm along their course (Di Pino *et al.* 2014). Three electrodes were implanted in each nerve. In detail, from distal to proximal, two intraneural ds-FILEs and one perineural *Cuff* electrode were inserted equally spaced at ∼10–15 cm above the elbow. The cables connected to the electrodes passed the skin through four different holes and were anchored to the skin on the anterior aspect of the arm.

ds-FILEs are custom-made multichannel electrodes (Fraunhofer Institute for Biomedical Engineering, St. Ingbert, Germany) with 16 active and two ground contacts arranged on both sides of a polyimide filament inserted within the nerve trunk (Poppendieck *et al.* 2015). Perineural *Cuff* electrodes (Ardiem Medical, East Indiana, PA, USA) are epineural multichannel electrodes with 14 active and two ground contacts, distributed on four rings wrapping the nerve trunk. A schematic representation of implants and arrangement of ds-FILE and *Cuff* contacts is given in Fig. 1.

Transcutaneous and invasive nerve stimulation

For transcutaneous stimulation, electrical pulses (constant current square wave pulses; duration, 200 μs) were applied through a bipolar electrode to the ulnar nerve above the elbow, by means of a Digitimer DS7A stimulator (Digitimer Ltd, Welwyn Garden City, UK). Anode and cathode were placed in the intermuscular sulcus, respectively 3 and 6 cm proximally from the centre of the line connecting the olecranon and the medial epicondyle.

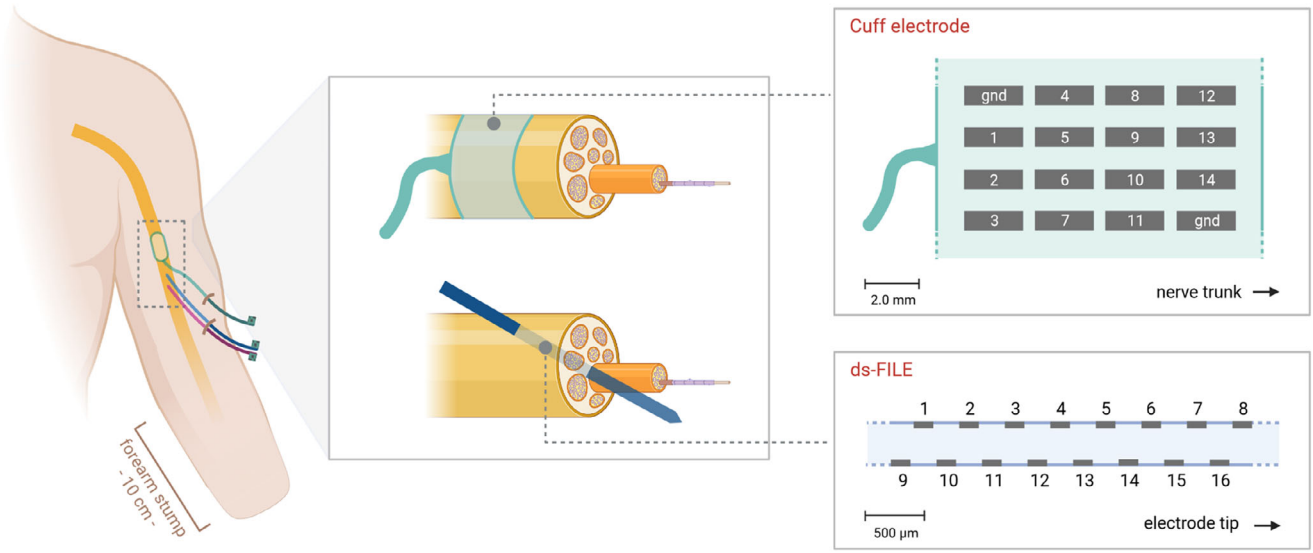

Figure 1. Schematic representation of ds-FILE and *Cuff* electrodes and their placement in the nerve trunk
Electrodes were implanted in the middle third of the left arm (left panel: a single nerve is represented). A *Cuff* electrode wraps the nerve trunk at a proximal site. Two ds-FILEs are inserted into the nerve trunk with an angle of approximately 45°. Active sites of the electrodes are represented in the right panels. The ds-FILE active area has a thickness of 360 μm and a total length of 3 mm and it bears 16 contacts (area: 150 × 50 μm^2), arranged on both sides of the electrode. [Image created with BioRender.com.] [Colour figure can be viewed at wileyonlinelibrary.com]

For invasive stimulation, electrical pulses were biphasic square-wave pulses, applied through the monopolar contacts of *Cuff* electrodes placed in the ulnar (CU) and median (CM) nerves and of an intraneural proximal ds-FILE placed in the median nerve (IM), by means of a STG4008 stimulator (Multi Channel Systems, Reutlingen, Germany). A dedicated stimulator was chosen to enable multichannel stimulation with low current intensity (output range: −16 to +16 mA) and with a high output resolution (intensity: 2000 nA; time: 20 μs), freely programmable in shape, intensity and duration. Stimulation parameters were chosen to inject a total charge below the safety limit for electrode and nerve damage, based on available data with similar electrodes (Dhillon *et al.* 2004; Dhillon, 2005; Rossini *et al.* 2010; Ortiz-Catalan *et al.* 2014; Tan *et al.* 2014). These parameters are within the range commonly used to stimulate peripheral nerves during micro-neurography investigations (Schady *et al.* 1983; Nannini & Horch, 1991). Attention was also paid to stimulate at a non-painful intensity in order to limit the recruitment of slow-conducting nociceptive afferent fibres.

Table 1. Sensory and motor thresholds for stimulation of individual contacts (indicated by numbers, as reported in Fig. 1) of the proximal median nerve intraneural electrode (IM) and median nerve *Cuff* electrode (CM)

IM contact	Sens. thr. (μA)	Motor thr. (μA)	CM contact	Sens. thr. (μA)	Motor thr. (μA)
IM1	120	–	CM1	150	150
IM2	350	–	CM2	200	300
IM3	300	–	CM3	300	400
IM4	300	–	CM4	150	250
IM5	200	–	CM5	200	250
IM6	–	–	CM6	150	250
IM7	350	–	CM7	200	250
IM8	300	–	CM8	250	250
IM9	80	–	CM9	–	–
IM10	100	–	CM10	–	–
IM11	50	–	CM11	200	250
IM12	100	–	CM12	250	250
IM13	300	–	CM13	300	250
IM14	160	200	CM14	200	250
IM15	150	200			
IM16	80	150			

Note that stimulation charge differs between IM and CM, since stimulus duration was 160 μs with IM contacts and 400 μs with CM contacts (total duration of biphasic square wave pulse).

Characterization of responses evoked by invasive nerve stimulation

To characterize the population of nerve fascicles activated by intraneural and perineural stimulation, we preliminarily mapped the motor responses and the perceived sensations by systematically recording sensory thresholds and compound muscle action potentials (CMAPs) evoked by stimulation through IM and CM contacts (Table 1). This was the only nerve with both perineural and intraneural electrodes available at the time of experiments.

As detailed in the Results section, all IM contacts (IM1–16) evoked somato-sensations referred to the area of the first three digits of the phantom hand, while only three distal IM contacts (IM14–16) also evoked recordable CMAPs. CM contacts were less selective and evoked both sensory perceptions and liminal CMAPs at sensory threshold or slightly higher intensities (Table 1). This preliminary mapping guided the choice of intraneural contacts used to deliver selective sensory afferent stimulation (IM10 and IM12) in the following SEP and SAI recordings.

SEP recordings

The participant lay on a bed, and she was instructed to stay awake with her eyes closed.

SEPs were recorded with a 32-channel BrainAmp amplifier (Brain Products, Gliching, Germany), using Ag/AgCl electrodes fixed to an elastic cap in the International 10−20 system locations. Scalp electrodes were referred to earlobe ipsilateral to the side of nerve stimulation. Signal was sampled at 5 kHz (bandpass: 0.5–2500 Hz; notch filter: 50 Hz) and digitized for offline analysis.

Peripheral stimulation was performed as transcutaneous electrical stimulation of the ulnar nerve of both sides and as intraneural stimulation of the left median nerve, as described above. Transcutaneous stimulation was delivered at just above the motor threshold intensity, so as to induce a small muscular twitch of the forearm muscle, at a frequency of 3.3 Hz. Intraneural stimulation was delivered by simultaneous activation of contacts 10 and 12 of the IM electrode, at an intensity of 2.0× the sensory threshold (200 μA; stimulus duration: 160 μs) and at a frequency of 3.3 Hz. These two IM contacts did not evoke motor responses in the tested stimulation intensity range (Table 1).

EEG signal processing was performed with the freely available EEGLab and Brainstorm Toolboxes software (Delorme & Makeig, 2004; Tadel *et al.* 2011). Preprocessing included: (a) removal of stimulation artefacts (cut stimulation artefacts) between −5 and 5 ms and interpolation of the signal; (b) band-pass filters between 0.3 and 300 Hz, 50 Hz notch filter; (c) independent component analysis-based removal of eye movements and muscular artefacts (Makeig *et al.* 2004); (d) extraction of EEG epochs; (e) direct current correction; (f) visual rejection

of epochs with remaining artefacts; (g) averaging of EEG epochs.

Source localization was performed taking into consideration the individual anatomical magnetic resonance imaging (MRI). To this aim a T1-weighted image was acquired. MRI segmentation and cortical reconstruction were performed with the Freesurfer toolbox (Dale *et al*. 1999). MRI data were imported into brainstorm where EEG data and MRI were co-registered, considering standard EEG electrode coordinates (10–20 system). A dipole fitting technique (ECD, equivalent current dipole) was applied, by using a single sphere forward model and assuming a brain conductivity value of 0.33 S/m for the brain (Bagić *et al*. 2011; Pellegrino *et al*. 2016*a*,*b*, 2018).

Over 2000 sweeps of whole-nerve stimulation and 7000 sweeps of intraneural stimulation were averaged for SEP analysis.

Transcranial magnetic stimulation (TMS)

TMS was performed with a Magstim 200^2 stimulator (Magstim Company Ltd, Whitland, UK). A figure-of-eight coil, with external loop diameters of 9 cm, was held over the motor cortex at the optimum scalp position to elicit MEPs in the contralateral target muscle. The coil was held tangentially to the scalp with the handle pointing backwards at an angle of approximately 45° to the mid-sagittal line, to generate an induced current with a posterior-to-anterior direction across the central sulcus.

MEPs were recorded from the following muscle targets of the upper limbs: biceps brachii (BB); ulnar-innervated forearm muscles (UFM), including flexor carpi ulnaris and flexor digitorum profundus; median-innervated forearm muscles (MFM), including pronator teres and flexor carpi radialis; and opponens pollicis (OP) of the intact side. Due to anatomical rearrangement of forearm stump muscles, muscular targets in the forearm were aided by surface EMG recordings of CMAPs generated by electrical stimulation of the ulnar and median nerves.

Resting motor threshold (RMT) was defined as the minimum stimulus intensity that produced a liminal MEP (>50 μV in at least 5 of 10 trials) at rest.

MEPs were recorded via two 9 mm diameter Ag-AgCl surface electrodes with the active electrode over the muscle belly and the reference electrode, respectively, on the muscle tendon at the elbow for the BB, on the ulnar bone for the forearm muscles (UFM and MFM) and on the interphalangeal joint of the 1st finger for the OP.

The EMG was amplified and filtered (bandwidth 3 Hz–3 kHz) by a Digitimer D360 amplifier (Digitimer). Data were stored on a computer with a sampling rate of 5 kHz per channel using a CED 1401 analogue-to-digital converter (Cambridge Electronic Design Ltd, Cambridge, UK).

Traces contaminated by muscle activation were discarded during acquisition. A few traces containing electrical artefacts or EMG activity due to voluntary muscle contraction were discarded after acquisition (six out of 450 acquired traces: $<2\%$).

Test of short-latency afferent inhibition (SAI)

We refer to short-latency afferent inhibition with the acronym SAI consistently with the TMS literature, and we alert the reader that in the present study SAI does not refer to slowly adapting type I afferent fibres.

SAI was studied using the paradigm described for transcutaneous nerve stimulation (Tokimura *et al*. 2000) and expressed as the ratio of the amplitude of MEPs conditioned by peripheral afferent stimulation and the amplitude of unconditioned MEPs. In the present experiments, conditioning electrical pulses were applied through implanted neural electrodes or bipolar skin electrodes (see section above).

Invasive stimulation was performed 30 days after the implantation of neural electrodes. Afferent stimuli were delivered through intraneural contacts IM12 and IM16 and perineural contacts CM5, CM14, CU5 and CU14 (Fig. 1). IM12 stimulation evoked a purely sensory perception, without evoked EMG activity, while IM16 stimulation was able to produce a recordable muscle activation together with tactile and proprioceptive perception, as in the case of *Cuff* contacts (Fig. 2*A*, detailed in the Results). The intensity of nerve stimulation was set at 2.0$\times$ the sensory threshold (stimulus duration: 160 μs). The intensity of the TMS test pulse over the motor cortex was adjusted to evoke an unconditioned MEP of $\sim$1.0 mV peak-to-peak amplitude in the relaxed target muscle. TMS target muscles were UFM for median nerve afferent stimulation and MFM for ulnar nerve afferent stimulation. We followed the principle of using target muscles innervated by a different nerve from the one used for afferent stimulation, since evoked responses in the agonist muscles are reported to have less SAI (Bertolasi *et al*. 1998).

In the case of transcutaneous mixed (sensory and motor) nerve stimulation, SAI was studied bilaterally. Recordings were performed 9 days after explantation of neural electrodes, when the bandage was removed from the left arm. Afferent stimuli were delivered to the ulnar nerve of both sides above the elbow, as described in the section above. The intensity of nerve stimulation was set at a level sufficient for evoking a just visible muscle contraction. TMS was targeted to the MFM hotspot on the scalp. MEPs were recorded simultaneously from relaxed BB, MFM and OP, to limit experimental time and test–retest variability. This approach is limited by the sub-optimal activation of cortical areas out of the hotspot or by cortico-cortical influences, although mitigated by the

overlapping of cortical representation maps of adjacent muscles (Krings *et al.* 1998; Raffin *et al.* 2015; DeJong *et al.* 2021) and by the presence of a within-test control intrinsic to the SAI measurement (i.e. the ratio of conditioned and unconditioned MEPs). RMTs, TMS intensity and test MEP amplitudes for both invasive and transcutaneous SAI protocols are reported in Table 2.

The peripheral conditioning stimulus preceded the TMS test pulse by inter-stimulus intervals (ISIs) that were related to the latency of the N20 component of the SEP by surface nerve stimulation; N20 peak latency was ∼17 ms. For transcutaneous stimulation, ISIs of N20+2, +3 and +4 ms (i.e. 19, 20 and 21 ms) were tested (10 randomized trials for each condition, 20 trials for the test condition).

In the case of invasive nerve stimulation, since no clear short-latency SEP was detectable with standard online analysis, ISIs were determined from the estimated peripheral-to-cortical conduction time based on stimulating electrode location. Specifically, the location of the stimulating electrode was ∼15 cm above the elbow in the case of invasive nerve stimulation (both intraneural and perineural), and 6 cm above the elbow in the case of the cathode used for transcutaneous stimulation. Given this different stimulating electrode location, the time needed for intraneural stimuli to reach the primary somatosensory cortex was estimated to be about 2 ms shorter than the N20 latency (i.e. 17 − 2 = 15 ms) recorded after transcutaneous stimulation. Therefore, ISIs

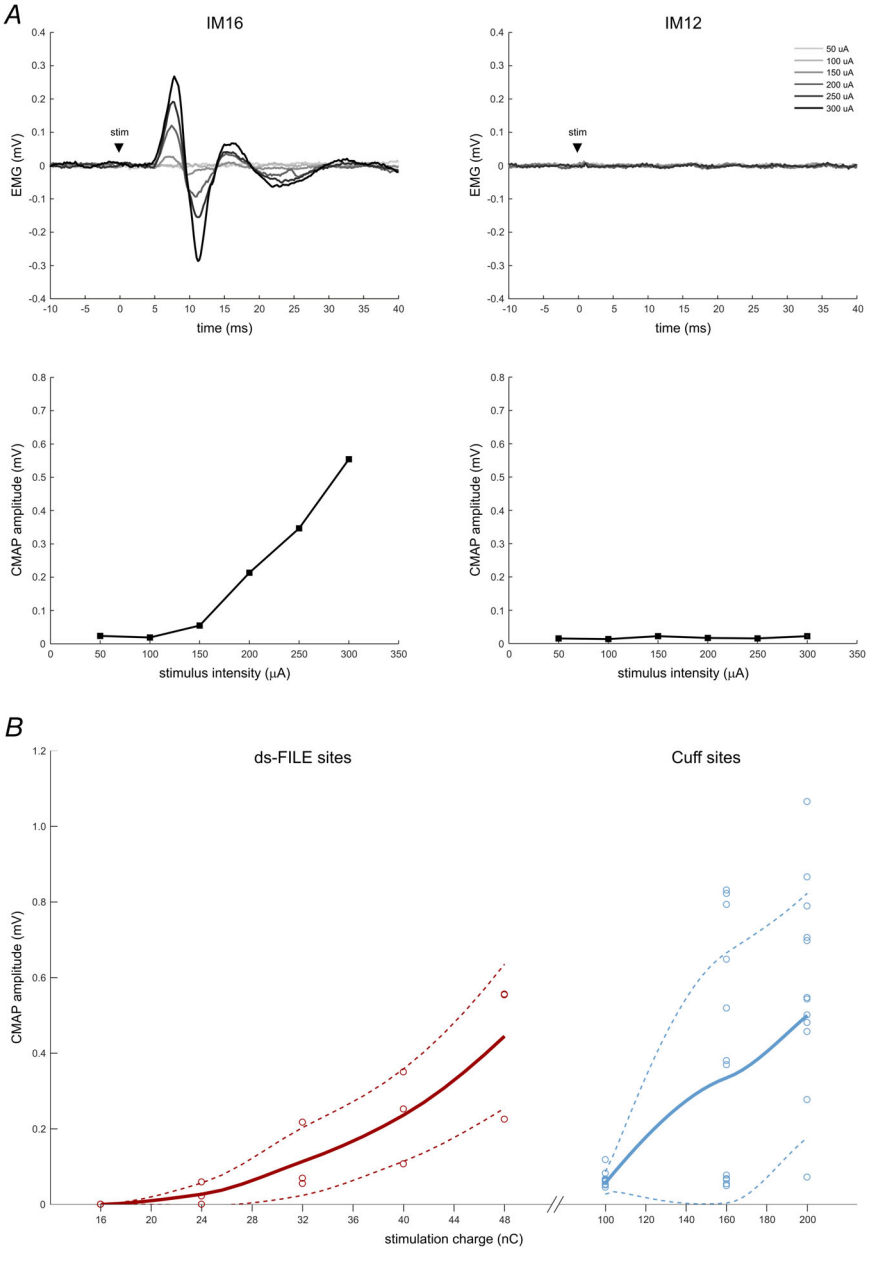

Figure 2. Recruitment of motor fibres with median nerve ds-FILE and *Cuff* electrode contacts
A, example of recruitment of compound muscle action potentials (CMAPs) after stimulation with IM16 and IM12 contacts at increasing intensities. At increasing stimulation intensities, IM16 elicits CMAPs of increasing amplitude (left panels); stimulation with IM12 does not evoke EMG responses in forearm muscles (right panels) while it evokes somatosensory perceptions and hence it is considered to be selective for sensory afferents. Each EMG trace (top panels) is the average of three trials. CMAP amplitude (bottom panels) is measured as peak-to-peak amplitude of the EMG signal. *B*, thick lines represent the average stimulus–response curves for tested contacts of ds-FILE (left curve, dark red) and *Cuff* (right curve, light blue) electrodes. Thin dashed lines represent the ±1 SD limits of the average curve. Circles represent the actual CMAPs (average of three stimuli). Curves are derived from actual and interpolated CMAPs obtained from contacts 14, 15 and 16 of the ds-FILE and from contacts 1–8 and 11–14 of the *Cuff* electrode, in the range of tested stimulation intensities. Contacts that did not evoke muscle responses are not represented. Stimulation was delivered as a biphasic square wave pulse, with a total duration of 160 μs for the ds-FILE and of 400 μs for the *Cuff* electrode contacts. Stimulation charge (nC) is calculated as stimulus intensity (μA) × duration (ms). Note the different charge scale for ds-FILE and *Cuff*. [Colour figure can be viewed at wileyonlinelibrary.com]

Table 2. Resting motor threshold (RMT), TMS intensity and test MEP amplitude for targeted upper limb muscles in invasive and transcutaneous SAI protocols

Afferent stim. site	Target muscle	RMT (% MSO)	TMS intensity (% MSO)	Test MEP (mV)
IM12	UFM.L	56	75	1.250
IM16	UFM.L			1.686
CM5	UFM.L			0.974
CM5+14	UFM.L			1.349
CU5	MFM.L	56	75	0.532
CU5+14	MFM.L			0.576
Ulnar	BB.L	60	84	0.682
(whole	MFM.L	60	84	1.063
nerve)*	BB.R	56	74	0.602
	MFM.R	56	74	1.388
	OP.R	n.a.	74	0.802

Abbreviations: MSO, maximum stimulator output; UFM, ulnar-innervated forearm muscles; MFM, median-innervated forearm muscles; BB, biceps brachii; OP, opponens pollicis; L/R, left/right side. See Methods and Fig. 1 for contact labelling details. RMT is measured by positioning the stimulating coil at the hotspot of each tested muscle.
*In the case of ulnar whole-nerve afferent stimulation, MEPs are co-recorded on each side after TMS at the MFM hotspot.

of 15–21 ms were tested (six randomized trials for each condition, 12 trials for the test condition). SAI is measured as the ratio of conditioned and unconditioned MEP amplitudes (i.e. an SAI value <1.0 indicates inhibition).

Measurements at ISIs of 19–21 ms (transcutaneous stimulation) and at ISIs of 15–16, 17–19 and 20–21 ms (invasive stimulation) were grouped for statistical analyses.

Statistical analysis

Statistical tests were applied to compare SAI values and other variables of interest between different experimental conditions. Since data distributions violated the assumptions of normality and/or homogeneity of groups, non-parametric statistics was applied. Boxplots of the distribution of collected data for different stimulation sites and ISIs are reported in the Results section. Between-group variance was tested by means of a Kruskal–Wallis test; when between-group analyses reported significant results, *post hoc* pairwise comparisons were performed by means of a Mann–Whitney test. P values of <0.05 were considered statistically significant. Since this is a single-case study with an exploratory nature and group differences were preliminarily assessed, pairwise tests were not corrected for multiple comparisons. Data were analysed using the software JASP for Windows v0.11.1 (The JASP Team, 2019).

Results

Characterization of responses evoked by invasive nerve stimulation

Following IM stimulation, at intensities between 50 and 400 μA (stimulus duration: 160 μs), all available electrode contacts (IM1–16) evoked somato-sensations (tactile/proprioceptive) referred to the area of the first three digits of the phantom hand. With stimulation intensities above sensory threshold, the more distal contacts (IM14–16) evoked also motor responses, recorded as CMAPs (Table 1; Fig. 2*A*).

Perineural stimulation through CM contacts, at intensities between 150 and 500 μA (stimulus duration: 400 μs), was less selective and evoked both sensory perceptions and liminal CMAPs at sensory threshold or slightly higher intensities with all available contacts (at the time of recordings, contacts IM6 and CM9 and 10 did not produce any sensory/motor response at the tested stimulation intensity range) (Table 1).

As expected, comparison of sensory thresholds between intraneural (n = 15) and perineural stimulation sites (n = 12) confirmed that thresholds were significantly lower with intraneural stimulation (U = 180.000, P < 0.0001) (Fig. 3). Concerning the activation of motor

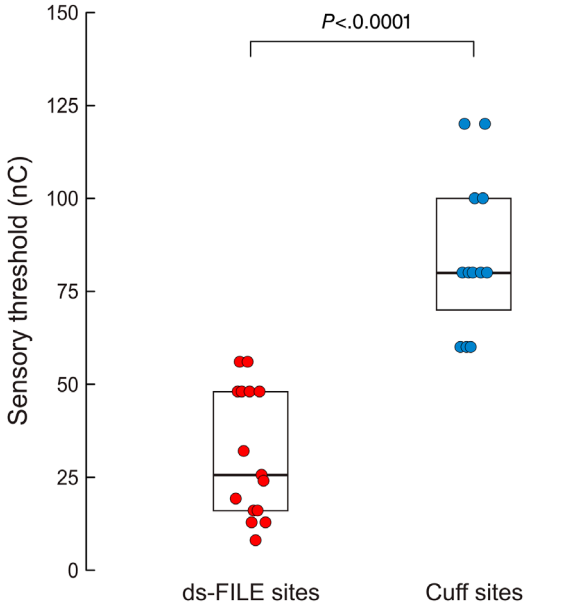

Figure 3. Comparison of sensory perception thresholds between median nerve ds-FILE and *Cuff* electrode contacts
Sensory thresholds for individual active sites evoking sensory perceptions within the tested stimulation range are represented. Threshold values are measured as stimulation charge, i.e. stimulation intensity (μA) × stimulus duration (ms). Boxplots summarize the lower quartile, median and upper quartile of the sample distribution for both electrodes. Thresholds with ds-FILE stimulation (n = 15) are significantly lower than with *Cuff* stimulation (n = 12) (P < 0.0001; Mann–Whitney test). [Colour figure can be viewed at wileyonlinelibrary.com]

fibres, stimulus–response curves show that stimulation with *Cuff* electrodes ($n = 12$), compared with intraneural stimulation ($n = 3$), requires higher intensities to elicit the same CMAP amplitude (Fig. 2*B*).

CU contacts were not systematically mapped by CMAP recording as several contacts (CU7–11) as well as the intraneural ulnar electrodes were not available at the time of experiments. However, all available CU contacts produced motor responses (detected as muscle twitches) at sensory threshold or higher stimulation intensity.

Somatosensory evoked potentials

Figure 4*A–C* shows the SEPs from transcutaneous left ulnar nerve stimulation, i.e. the amputated side. Figure 4*A* shows the time course of all EEG channels ('butterfly plot'). The first cortical response is at ∼17 ms and has a typical bipolar topographical distribution (Fig. 4*B*). Source localization performed with the dipole fitting technique (Fig. 4*C*) localized a dipole at the bottom of the right central sulcus, next to the hand area representation

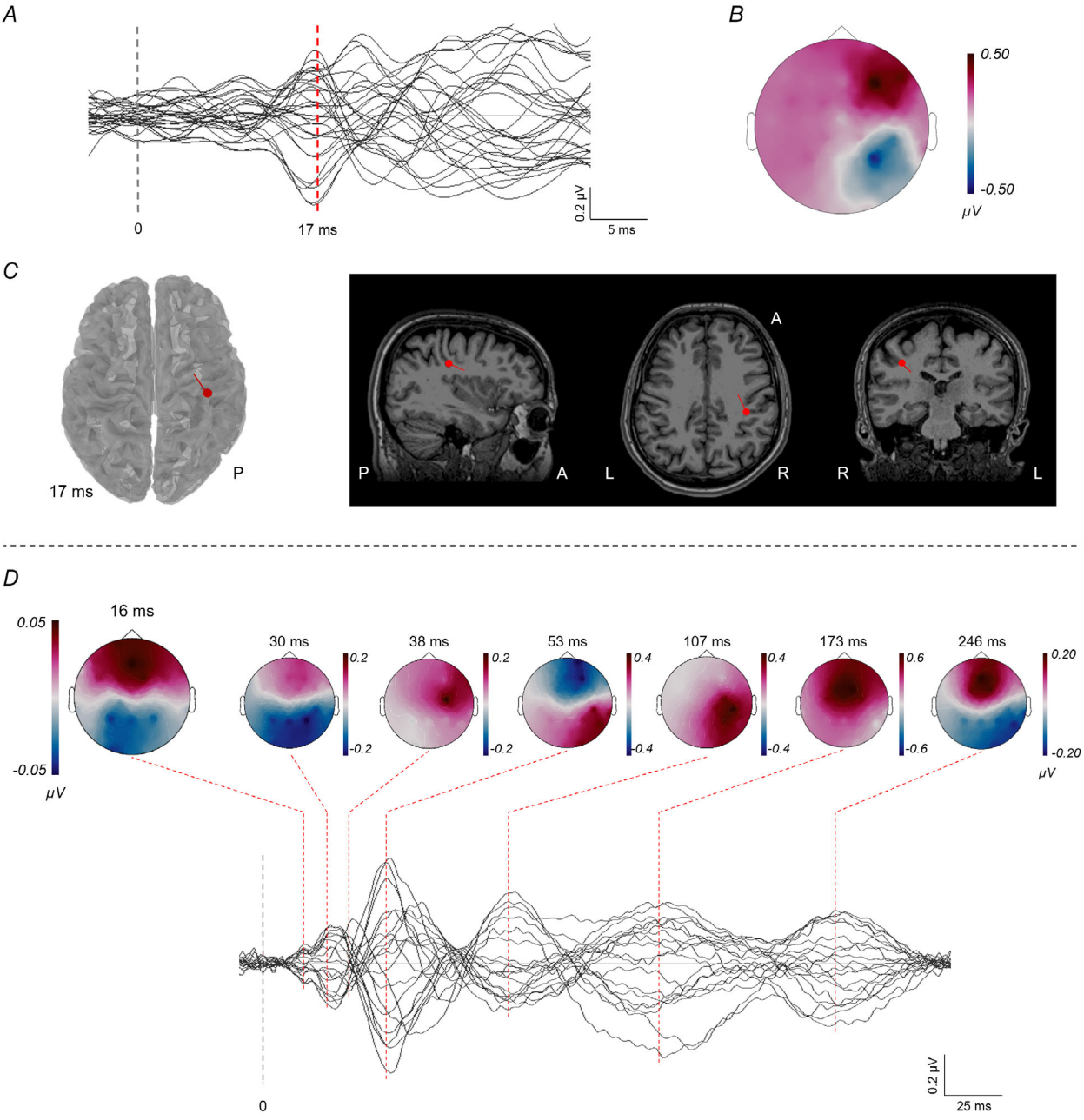

Figure 4. Somatosensory evoked potentials from transcutaneous left ulnar nerve stimulation (*A–C*) and from left intraneural median nerve stimulation (*D*)
See Results for details. [Colour figure can be viewed at wileyonlinelibrary.com]

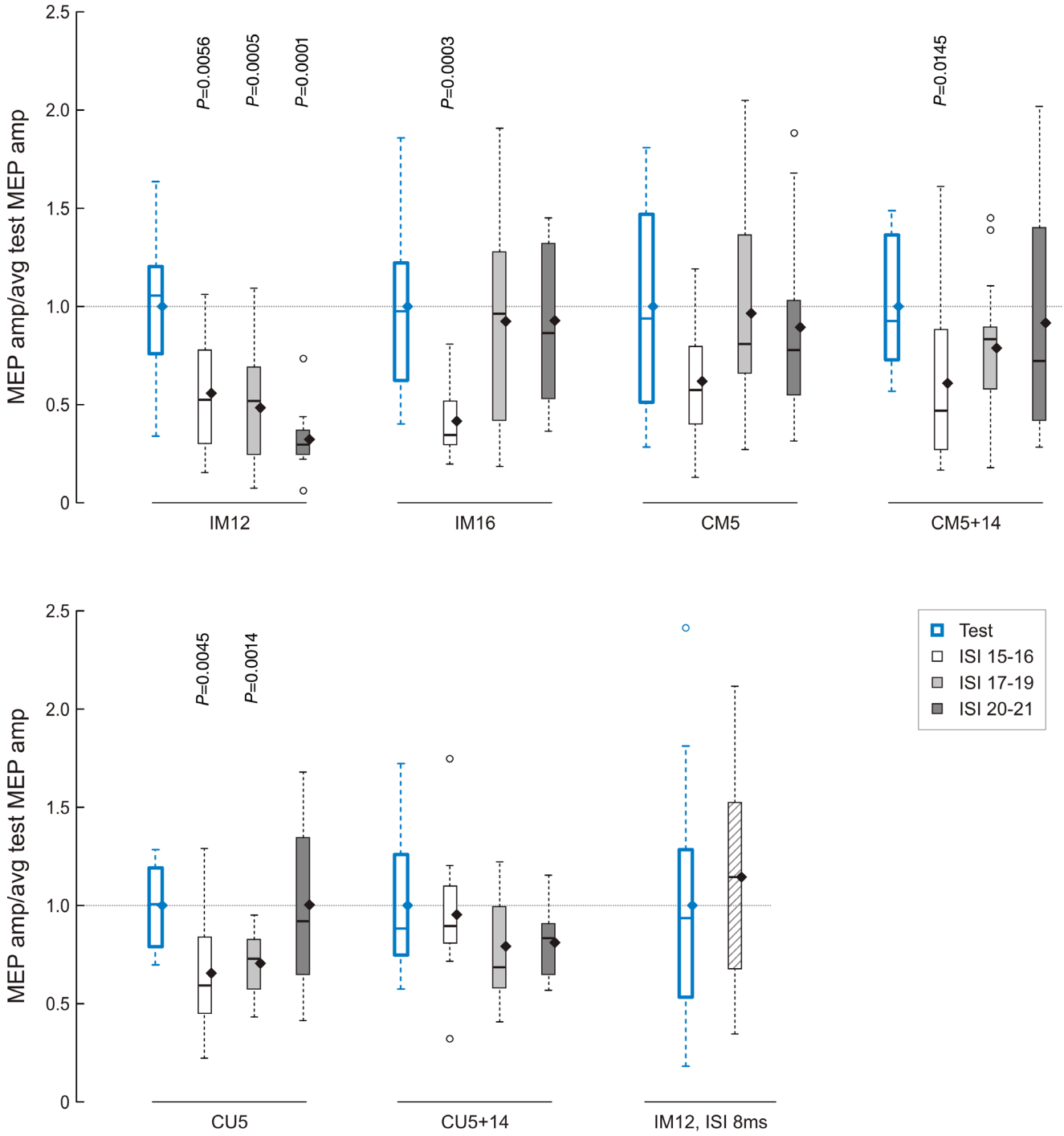

Figure 5. SAI values obtained by delivering the conditioning afferent pulse with different electrodes and contacts, at different inter-stimulus intervals (ISIs)
Boxplots represent MEP amplitudes by single pulse TMS (test condition, $n = 12$) and by paired pulse TMS, normalized to the average test MEP amplitude ($n = 6$ for each ISI). All stimulation sites of ds-FILE and *Cuff* electrodes are associated with a reduction of the test MEP amplitude in the target muscle across tested ISIs from 15 to 21 ms (i.e. SAI < 1.0). SAI was analysed by grouping ISIs of 15–16 ms (white boxes), 17–19 ms (light grey) and 20–21 ms (dark grey). The ISI of 8 ms ($n = 14$) was used as a control condition that is not expected to generate SAI. Boxplots represent the lower quartile, median and upper quartile of the sample distribution; whiskers extend up to 1.5 times the interquartile range; circles indicate outliers; and black diamonds indicate the mean of the sample. Significant *P* values of comparisons between conditioned and test MEPs (Mann–Whitney tests) are reported. [Colour figure can be viewed at wileyonlinelibrary.com]

(hand knob). Overall, transcutaneous SEP generated a clear and well-reproducible first cortical response, which localized in the right central region. Right ulnar nerve stimulation (i.e. the intact side) evoked cortical responses with the same latency of SEP recorded after left side stimulation.

Figure 4*D* shows the SEPs obtained with intraneural median nerve stimulation, with a time course until 300 ms. The first cortical response is recognizable at ∼16 ms. The amplitude of this response is about six times smaller than that of the compound SEP from whole-nerve stimulation. The signal to noise ratio is low so that no reliable source localization could be performed. The later latencies show the typical SEP pattern, with a high-amplitude response, and multiple polarity inversions over time (see topographical distribution).

Afferent inhibition by invasive nerve stimulation

Conditioning afferent stimuli were delivered through intraneural contacts IM12 and IM16 and perineural contacts CM5, CM14, CU5 and CU14. IM12 stimulation evoked a purely sensory perception, without evoked EMG activity, while IM16 stimulation produced a recordable muscle activation together with tactile and proprioceptive perception (Fig. 2*A*).

As a first step, we performed an exploratory analysis across tested ISIs and stimulation sites. Figure 5 shows that all stimulation sites of perineural and intraneural electrodes were associated with a reduction of the test MEP amplitude in the target muscle across tested ISIs from 15 to 21 ms (i.e. SAI < 1.0), and pooled analysis comparing conditioned ($n = 246$) and test MEP amplitudes ($n = 72$) revealed significant inhibition of conditioned responses [median: 0.71, interquartile range (IQR): 0.53, $U = 12282.500$, $P < 0.0001$]. Moreover, IM12 was the site that produced the largest and significant inhibition of ∼50% of the average test MEP throughout the tested ISI range of 15–21 ms, while other sites resulted in a variable amount of inhibition, predominantly at shorter ISIs (Fig. 5). A control trial with IM12 conditioning at the ISI of 8 ms produced no MEP inhibition (median: 1.14, IQR: 0.81, $N = 26$, $U = 70.000$, $P = 0.494$) (Fig. 5).

SAI was significantly affected by the site of afferent stimulation ($N = 246$; six levels: IM12, IM16, CM5, CM5+14, CU5 and CU5+14; Kruskal–Wallis test: $H_5 = 32.362$, $P < 0.0001$), indicating that a different amount of inhibition is produced by different stimulation sites (Fig. 6*A*). Pairwise comparisons show that SAI produced by IM12 conditioning (i.e. selective sensory afferent fibre stimulation) ($n = 42$) was significantly

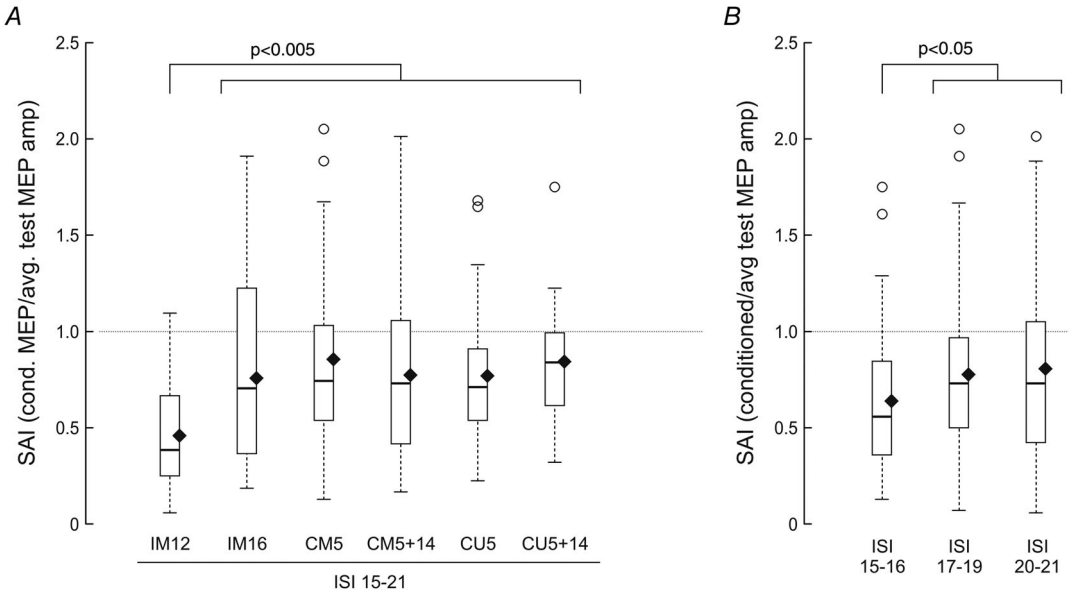

Figure 6. Effect of stimulation site and ISI on SAI
A, effect of stimulation site on SAI. Boxplots represent SAI values obtained by delivering the conditioning afferent pulse with different electrodes and contacts, by grouping ISIs of 15–21 ms. *P* values indicate significant differences for each site compared with IM12 (Mann–Whitney tests; individual *P* values reported in the Results). *B*, effect of ISI on SAI. Boxplots represent SAI values obtained by delivering the conditioning afferent pulse at different ISIs, by grouping all contacts indicated in *A*. *P* values indicate significant differences for each ISI compared with the ISI of 15–16 ms (Mann–Whitney tests; individual *P* values reported in the Results). SAI values below 1.0 indicate inhibition of the test MEP. Boxplots represent the lower quartile, median and upper quartile of the sample distribution; whiskers extend up to 1.5 times the interquartile range; circles indicate outliers; and black diamonds indicate the mean of the sample.

larger than SAI produced by non-selective stimulation (SAI_{IM16}: $n = 40$, $U = 491.000$, $P = 0.0010$; SAI_{CM5}: $n = 39$, $U = 1276.000$, $P < 0.0001$; SAI_{CM5+14}: $n = 42$, $U = 1257.000$, $P = 0.0007$; SAI_{CU5}: $n = 41$, $U = 1326.000$, $P < 0.0001$; SAI_{CU5+14}: $n = 42$, $U = 1476.000$, $P < 0.0001$) (Fig. 6*A*).

SAI was also affected by the ISI ($N = 246$; three levels: ISI15–16, ISI17–19 and ISI20–21; Kruskal–Wallis test: $H_2 = 6.574$, $P = 0.0374$). Pairwise comparisons show that pooled SAI from all stimulation sites at ISI15–16 ($n = 69$) was significantly larger than SAI at ISI17–19 ($n = 108$, $U = 2933.000$, $P = 0.0171$) and at ISI20–21 ($n = 69$, $U = 1888.000$, $P = 0.0362$) (Fig. 6*B*).

Afferent inhibition by transcutaneous nerve stimulation

Surface stimulation of the left (amputated side) and of the right ulnar nerve at the elbow inhibited MEPs from the contralateral motor cortices, at ISIs from 19 to 21 ms (i.e. N20+2, +3 and +4 ms). The inhibition of the test response is evident in all tested muscles: BB and MFM of both sides and right OP (Fig. 7).

SAI in the left MFM ($n = 30$) was comparable to that obtained in the same muscle and at the same relative ISIs after invasive stimulation of the ulnar nerve with the *Cuff* electrode (median: 0.69 *vs.* 0.73 with CU5, $n = 41$, $P = 0.591$, and 0.68 with CU5+14, $n = 42$, $P = 0.620$).

Kruskal–Wallis tests showed that SAI was significantly affected by the side of afferent stimulation ($N = 120$; two levels: right, left; $H_1 = 40.067$, $P < 0.0001$), but not by the muscle being tested ($N = 120$; two levels: BB, MFM; $H_1 = 0.834$, $P = 0.361$). At *post hoc* comparisons, SAI was significantly more pronounced on the right (intact) side for both BB ($N = 60$, $U = 682.000$, $P = 0.0005$) and MFM ($N = 60$, $U = 807.000$, $P < 0.0001$).

Moreover, SAI was measured in the OP muscle of the intact side: SAI was not significantly different between hand (OP, median: 0.45), forearm (MFM, median: 0.39) and arm (BB, median: 0.48) muscles of the intact side ($N = 90$, H_2: 5.011, $P = 0.0816$) (Fig. 7).

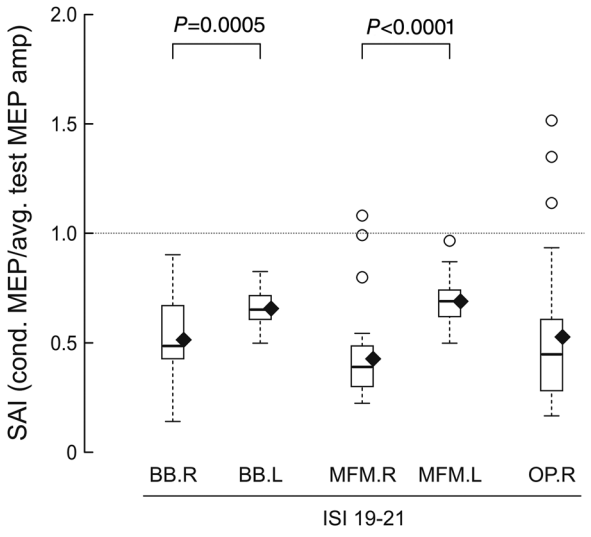

Figure 7. Boxplots of SAI values obtained in different muscles of the right (intact) and left (amputated) side after conditioning by transcutaneous ulnar nerve stimulation at the elbow
Values below 1.0 indicate inhibition of the test MEP. SAI was analysed by grouping ISIs of 19–21 ms. SAI is significantly lower for muscles of the amputated side (Mann–Whitney tests). Boxplots represent the lower quartile, median and upper quartile of the sample distribution; whiskers extend up to 1.5 times the interquartile range; circles indicate outliers; and black diamonds indicate the mean of the sample.

Discussion

In the present experiments, we exploited intraneural and perineural electrodes implanted for prosthesis control to investigate the physiological mechanisms of interaction of selective somatosensory afferents with sensorimotor cortical circuits. Afferent somatosensory input mediates tactile, proprioceptive and haptic perception and, for this reason, it is crucial for the correct execution of purposeful goal-directed movements. In this context, afferent inhibition of motor output might represent a long reflex mechanism contributing to the precise tuning of muscle activation/suppression during fine motor tasks.

Peripheral feedback through different sensory modalities, using both non-invasive and invasive stimulation methods, has been used to improve manipulation skills of hand prostheses.

Moreover, techniques that exploit sensorimotor integration, with approaches based on 'task-intrinsic' or 'augmented feedback', have been proposed to potentiate impaired afferent pathways and to foster the recovery of motor function in the rehabilitation of different neurological conditions involving the central (Molier *et al.* 2010; Abbruzzese *et al.* 2014; Hayward *et al.* 2014; Edwards *et al.* 2019) or the peripheral nervous system (Gordt *et al.* 2018; Oddsson *et al.* 2020).

As a first step, we examined selectivity of stimulation through neural interfaces by mapping sensory perceptions and motor responses. Median nerve stimulation through intraneural contacts evoked tactile/proprioceptive perceptions referred to the area of the first three digits at all stimulating sites, while only three contacts of the electrode evoked motor responses within the tested stimulation intensity range. Median nerve stimulation through perineural contacts was less selective: all contacts evoked both sensory perceptions and muscle responses at intensities of stimulation near sensory threshold (Table 1; Fig. 2), probably because of the location of active sites over

the epineurium. In the present experiments, a limiting factor in the determination of selectivity of intraneural stimulation on sensory afferents relates to the fact that we did not discriminate between skin and muscle afferents by means of microneurographic recordings. However, it can be hypothesized that both components were activated by afferent stimulation at 2.0× sensory threshold intensity used in SEP and SAI recordings, also based on the subject's perceived sensations.

SEP recording allowed us to detect cortical areas activated by transcutaneous and intraneural stimulation. Transcutaneous stimulation of the ulnar nerve just above the elbow evoked cortical responses in the parietal area with a peak latency of about 17 ms, that is within a normal range, confirming the physiological recruitment and integrity of somatosensory afferent pathways. These data are in line with previous reports of preserved responsiveness of S1 after long-term deafferentation in arm amputees, albeit with diminished amplitude (Mackert *et al*. 2003). Intraneural stimulation evoked a less reproducible cortical activation in the parietal area that was clearly detectable by averaging a large number of trials (>7000), with a peak latency of the earliest SEP component of about 16 ms; this latency is compatible with the activation of fast-conducting afferent fibres at the stimulation site located in the middle third of the arm. The amplitude of this early cortical response to intraneural stimulation was about six times smaller than that of the compound SEP from whole-nerve stimulation. These data confirm that intraneural stimulation was effective in activating S1. However, the stimulation intensity of 2.0× the sensory threshold probably produced a submaximal activation of large-diameter somatic afferent fibres that might account for the reduced amplitude of cortical responses compared with compound nerve stimulation, in agreement with findings of previous microstimulation experiments (Kunesh *et al*. 1995). It should also be noted that it is unclear whether the short-latency parietal SEP component reflects the activity of a single cortical generator, since the thalamic relay is distributed to several post-central areas (3b, 1 and 2) within S1 (Allison 1982; Eisen 1982). While this interpretation is compatible with findings of initial reports on SEPs evoked by stimulation modalities with different fibre selectivity in healthy subjects (Pratt *et al*. 1979; Cohen *et al*. 1985), it is not sufficiently supported by data of previous reports that documented parietal cortical activation following intraneural stimulation in trans-radial amputees. In the latter case, a higher intensity of stimulation, eliciting the strongest non-painful sensation, evoked low-amplitude cortical responses (Granata *et al*. 2018) and stimulation delivered through multiple contacts did not facilitate SEPs (Strauss *et al*. 2019). An alternative explanation is that reduced SEP amplitude/persistence is due to functional reorganization of cortical circuitry in chronic amputation (Mackert *et al*. 2003; Di Pino *et al*. 2009, 2021). Nonetheless, these data strongly suggest that the specific perception of the artificial sensory stimuli elicited by peripheral nerve stimulation and reported by the subjects in their phantom of the hand involves the activation of the S1 hand area.

Testing the MEP afferent inhibition allowed us to investigate the integration of sensory afferents with motor cortical efferent circuits. The phenomenon of SAI has been extensively explored using surface mixed nerve stimulation and it exhibits inhibition of M1 output at short ISIs of N20 latency + 0–8 ms, it being more pronounced at ISIs of N20 latency + 0–4 ms (Tokimura *et al*. 2000). In our participant, transcutaneous nerve stimulation produced an SAI effect on M1 coherent with data reported in the literature. It is worth noting that we observed a reduced inhibition of M1 output to stump muscles compared with the contralateral M1 (Fig. 7). This finding could account for increased excitability of cortical areas controlling proximal muscles of the amputated limb (Cohen *et al*. 1991; Pascual-Leone *et al*. 1996; Röricht *et al*. 1999). However, in our subject we did not observe an overt imbalance of motor thresholds supporting increased corticospinal excitability in the amputated side; therefore, an alternative explanation is that, since the amount of SAI has been shown to correlate with that of S1 activation (Bailey *et al*. 2016), reduced inhibition of the affected side might depend on reduced activation of deafferented S1 (Marckert *et al*. 2003). Moreover, when comparing SAI from the amputated and intact side, it must be taken into account that, in our subject, the prolonged period of sensorimotor training with prosthesis might have influenced the level of sensorimotor cortical excitability, and hence the amount of MEP inhibition in stump muscles (Zollo *et al*. 2019).

In our study, we tested for the first time the SAI effect produced by conditioning stimuli delivered through invasive neural interfaces. After stimulation with both perineural and intraneural electrodes, we demonstrated suppression of M1 response to TMS at ISIs compatible with a cortical effect of afferent stimuli. As shown in Figs 5 and 6, the ISIs generating suppression of MEPs with intraneural/perineural stimulation (tested in the range from N20 + 0–6 ms) are in the same range of those generating suppression of MEPs with surface stimulation (tested in the range from N20 + 2–4 ms, Fig. 7). The interval-specific effect of intraneural stimulation is confirmed by the absence of inhibition at an ISI of 8 ms, which is shorter than the time needed for the afferent stimulus to reach S1 (Fig. 5). Moreover, we observed a significantly stronger SAI by delivering afferent stimuli through one intraneural contact (IM12) that was selective for sensory fibres (Fig. 6), as this contact did not activate motor fibres at intensities of stimulation tested up to ∼3.0× the sensory threshold (Fig. 2*A*). This finding is

in agreement with the interpretation that tactile sensory fibres activating thalamo-cortical afferents are specifically involved in the origin of suppression of M1 excitability. Indeed, intraneural or perineural contacts that were not selective for sensory fibres, and hence are likely to have activated a reduced pool of tactile afferent fibres, produced a weaker conditioning of M1 (Fig. 6). This interpretation would agree with findings of Bailey *et al.* (2016), who reported that the amount of SAI depends on the volume of the sensory afferent volley to S1 and that it ceases to increase once all afferent fibres within the nerve are recruited. It remains to be interpreted why the stimulation delivered by activating simultaneously two *Cuff* contacts on either median or ulnar nerve, which should recruit a larger pool of fibres, was not more efficacious in producing SAI (Fig. 6). This might be explained by previous findings showing that afferent inputs from larger cutaneous receptive fields produce less SAI (Tamburin *et al.* 2005), possibly due to centre-surround inhibition mechanisms (Dubbioso *et al.* 2017). This finding also agrees with the lack of SEP facilitation by stimulation from multiple intraneural contacts (Strauss *et al.* 2019). A possible explanation is also that sensory afferents with a different somatotopic distribution within the nerve trunk might have a different functional role in movement shaping, and hence be differentially involved in the SAI effect. Additionally, interference with the SAI effect due to recruitment of a larger pool of muscle afferents cannot be ruled out, since some data support the hypothesis of a predominant contribution of cutaneous afferents to SAI (Pilurzi *et al.* 2020).

Which cortical circuit is primarily responsible for the origin of SAI is still a matter of debate: the main hypotheses are that SAI is generated by cortico-cortical connections from S1 to M1 or by suppression of facilitatory thalamic afferents to M1 (Tokimura *et al.* 2000). Moreover, pharmacological studies indicate that the phenomenon of SAI requires the physiological activity of central cholinergic projections (Di Lazzaro *et al.* 2000), possibly to cortical GABAergic interneurons (Xiang *et al.* 1998; Di Lazzaro *et al.* 2007; Kruglikov & Rudy, 2008).

With both intraneural and perineural conditioning stimulation, we observed the strongest SAI at ISIs of 15–16 ms (Fig. 6*B*), which correspond to the shortest latency of parietal cortical activation after peripheral nerve stimulation documented by SEP recordings (Fig. 4*D*). This very short latency effect is in agreement with previous findings of afferent inhibition at ISIs corresponding to the time of the N20 peak latency (Bertolasi *et al.* 1998; Benussi *et al.* 2020) and could be interpreted as an inhibitory mechanism at the level of direct thalamic projections to M1. However, SAI at shorter ISIs is still compatible with sensorimotor cortico-cortical interactions, if we take into account two physiological mechanisms: (1) the reference of the N20 peak latency probably represents a later phase of S1 activation, onset of which might be 1—2 ms earlier, as also demonstrated by high-frequency oscillations of the cortical SEP (Ozaki & Hashimoto 2011) – this is compatible with a sensory conduction time shorter than the earliest ISI producing M1 inhibition; and (2) SAI depends on suppression of the later components of the corticospinal descending volley generated by focal TMS of M1 (Tokimura *et al.* 2000) that are delayed ∼3 ms or more relative to direct activation of corticospinal cells (Di Lazzaro *et al.* 2012).

Since the present results come from a case study, we must point out that extension beyond our subject of some of our findings should be done with caution. Indeed, the main finding is that selective sensory fascicle stimulation is able to evoke a detectable activity in S1 and to produce an SAI effect in M1, and this could be employed as a physiological basis for further developments of intraneural stimulation and prosthesis control strategies. However, the more specific results related to the different amount of SAI due to the location of implanted active sites and to the timing of afferent stimulation, as well as SEP morphology, might be individual characteristics and might not be confirmed in the general population.

Conclusions

(1) We confirm that multichannel intraneural electrodes of the ds-FILE type are effective in producing selective sensory and motor nerve fascicle stimulation.
(2) Cortical activity in S1 can be evoked by selective stimulation of sensory fibres in humans. The reduced amplitude of SEPs evoked by this type of stimulation compared with SEPs evoked by surface mixed nerve stimulation might reflect submaximal activation of large-diameter afferent fibres and de-synchronized activation of cortical cell populations. This opens up the intriguing hypothesis that the activation of S1 we are typically accustomed to see in SEP may be an artefactual signal due to the synchronous hyperactivation of the whole nerve, which does not occur during the physiological somatosensory stimulation of the hand in the everyday interaction with objects. Rearrangement of afferent pathways or cortical circuitry related to chronic amputation could also have influenced SEP amplitude and persistence.
(3) For the first time, we demonstrate the possibility of generating inhibition of motor cortical output by perineural and intraneural conditioning stimulation at short ISIs, more prominently by selective stimulation of somatosensory afferent fibres: this supports the existence of a fast sensorimotor integration process, probably mediated by thalamo-cortical afferents.

References

Abbruzzese G, Trompetto C, Mori L & Pelosin E (2014). Proprioceptive rehabilitation of upper limb dysfunction in movement disorders: a clinical perspective. *Front Hum Neurosci* **8**, 961.

Allison T (1982). Scalp and cortical recordings of initial somatosensory cortex activity to median nerve stimulation in man. *Ann N Y Acad Sci* **388**, 671–678.

Bagić AI, Knowlton RC, Rose DF, Ebersole JS & ACMEGS Clinical Practice Guideline (CPG) Committee (2011). American clinical magnetoencephalography society clinical practice guideline 1: recording and analysis of spontaneous cerebral activity. *J Clin Neurophysiol* **28**, 348–354.

Bailey AZ, Asmussen MJ & Nelson AJ (2016). Short-latency afferent inhibition determined by the sensory afferent volley. *J Neurophysiol* **116**, 637–644.

Benussi A, Grassi M, Palluzzi F, Koch G, Di Lazzaro V, Nardone R, Cantoni V, Dell'Era V, Premi E, Martorana A, di Lorenzo F, Bonnì S, Ranieri F, Capone F, Musumeci G, Cotelli MS, Padovani A & Borroni B (2020). Classification accuracy of transcranial magnetic stimulation for the diagnosis of neurodegenerative dementias. *Ann Neurol* **87**, 394–404.

Bertolasi L, Priori A, Tinazzi M, Bertasi V & Rothwell JC (1998). Inhibitory action of forearm flexor muscle afferents on corticospinal outputs to antagonist muscles in humans. *J Physiol* **511**, 947–956.

Ciancio AL, Cordella F, Barone R, Romeo RA, Bellingegni AD, Sacchetti R, Davalli A, Di Pino G, Ranieri F, Di Lazzaro V, Guglielmelli E & Zollo L (2016). Control of prosthetic hands via the peripheral nervous system. *Front Neurosci* **10**, 116.

Cohen LG, Starr A & Pratt H (1985). Cerebral somatosensory potentials evoked by muscle stretch, cutaneous taps and electrical stimulation of peripheral nerves in the lower limbs in man. *Brain* **108**, 103–121.

Cohen LG, Bandinelli S, Findley TW & Hallett M (1991). Motor reorganization after upper limb amputation in man. A study with focal magnetic stimulation. *Brain* **114**, 615–627.

Cutrone A & Micera S (2019). Implantable neural interfaces and wearable tactile systems for bidirectional neuroprosthetics systems. *Adv Healthc Mater* **8**, 1801345.

D'Anna E, Valle G, Mazzoni A, Strauss I, Iberite F, Patton J, Petrini FM, Raspopovic S, Granata G, Di Iorio R, Controzzi M, Cipriani C, Stieglitz T, Rossini PM & Micera S (2019). A closed-loop hand prosthesis with simultaneous intraneural tactile and position feedback. *Sci Robot* **4**, eaau8892.

Dale AM, Fischl B & Sereno MI (1999). Cortical surface-based analysis. I. Segmentation and surface reconstruction. *Neuroimage* **9**, 179–194.

DeJong SL, Bisson JA, Darling WG & Shields RK (2021). Simultaneous recording of motor evoked potentials in hand, wrist and arm muscles to assess corticospinal divergence. *Brain Topogr* **34**, 415–429.

Delorme A & Makeig S (2004). EEGLAB: an open source toolbox for analysis of single-trial EEG dynamics including independent component analysis. *J Neurosci Methods* **134**, 9–21.

Dhillon GS, Lawrence SM, Hutchinson DT & Horch KW (2004). Residual function in peripheral nerve stumps of amputees: Implications for neural control of artificial limbs. *J Hand Surg* **29**, 605–615.

Dhillon GS (2005). Effects of short-term training on sensory and motor function in severed nerves of long-term human amputees. *J Neurophysiol* **93**, 2625–2633.

Di Lazzaro V, Oliviero A, Profice P, Pennisi MA, Di Giovanni S, Zito G, Tonali P & Rothwell JC (2000). Muscarinic receptor blockade has differential effects on the excitability of intracortical circuits in the human motor cortex. *Exp Brain Res* **135**, 455–461.

Di Lazzaro V, Pilato F, Dileone M, Profice P, Ranieri F, Ricci V, Bria P, Tonali PA & Ziemann U (2007). Segregating two inhibitory circuits in human motor cortex at the level of $GABA_A$ receptor subtypes: a TMS study. *Clin Neurophysiol* **118**, 2207–2214.

Di Lazzaro V, Profice P, Ranieri F, Capone F, Dileone M, Oliviero A & Pilato F (2012). I-wave origin and modulation. *Brain Stimul* **5**, 512–525.

Di Pino G, Guglielmelli E & Rossini PM (2009). Neuroplasticity in amputees: main implications on bidirectional interfacing of cybernetic hand prostheses. *Prog Neurobiol* **88**, 114–126.

Di Pino G, Porcaro C, Tombini M, Assenza G, Pellegrino G, Tecchio F & Rossini PM (2012). A neurally-interfaced hand prosthesis tuned inter-hemispheric communication. *Restor Neurol Neurosci* **30**, 407–418.

Di Pino G, Denaro L, Vadalà G, Marinozzi A, Tombini M, Ferreri F, Papalia R, Accoto D, Guglielmelli E, Di Lazzaro V & Denaro V (2014). Invasive neural interfaces: the perspective of the surgeon. *J Surg Res* **188**, 77–87.

Di Pino G, Romano D, Spaccasassi C, Mioli A, D'Alonzo M, Sacchetti R, Guglielmelli E, Zollo L, Di Lazzaro V, Denaro V & Maravita A (2020). Sensory- and action-oriented embodiment of neurally-interfaced robotic hand prostheses. *Front Neurosci* **14**, 389.

Di Pino G, Piombino V, Carassiti M & Ortiz-Catalan M (2021). Neurophysiological models of phantom limb pain: what can be learnt. *Minerva Anestesiol* **87**, 481–487.

Dubbioso R, Raffin E, Karabanov A, Thielscher A & Siebner HR (2017). Centre-surround organization of fast sensorimotor integration in human motor hand area. *Neuroimage* **158**, 37–47.

Dubbioso R, Manganelli F, Siebner HR & Di Lazzaro V (2019). Fast intracortical sensory-motor integration: a window into the pathophysiology of Parkinson's disease. *Front Hum Neurosci* **13**, 111.

Edwards LL, King EM, Buetefisch CM & Borich MR (2019). Putting the "sensory" into sensorimotor control: the role of sensorimotor integration in goal-directed hand movements after stroke. *Front Integr Neurosci* **13**, 16.

Eisen A (1982). The somatosensory evoked potential. *Can J Neurol Sci* **9**, 65–77.

Ferreri F, Ponzo D, Vollero L, Guerra A, Di Pino G, Petrichella S, Benvenuto A, Tombini M, Rossini L, Denaro L, Micera S, Iannello G, Guglielmelli E, Denaro V & Rossini PM (2014). Does an intraneural interface short-term implant for robotic hand control modulate sensorimotor cortical integration? An EEG-TMS co-registration study on a human amputee. *Restor Neurol Neurosci* **32**, 281–292.

Gordt K, Gerhardy T, Najafi B & Schwenk M (2018). Effects of wearable sensor-based balance and gait training on balance, gait, and functional performance in healthy and patient populations: a systematic review and meta-analysis of randomized controlled trials. *Gerontology* **64**, 74–89.

Gori M, Vadalà G, Giannitelli SM, Denaro V & Di Pino G (2021). Biomedical and tissue engineering strategies to control foreign body reaction to invasive neural electrodes. *Front Bioeng Biotechnol* **9**, 659033.

Granata G, Di Iorio R, Romanello R, Iodice F, Raspopovic S, Petrini F, Strauss I, Valle G, Stieglitz T, Čvančara P, Andreu D, Divoux JL, Guiraud D, Wauters L, Hiairrassary A, Jensen W, Micera S & Rossini PM (2018). Phantom somatosensory evoked potentials following selective intraneural electrical stimulation in two amputees. *Clin Neurophysiol* **129**, 1117–1120.

Hayward KS, Barker RN, Carson RG & Brauer SG (2014). The effect of altering a single component of a rehabilitation programme on the functional recovery of stroke patients: a systematic review and meta-analysis. *Clin Rehabil* **28**, 107–117.

Hooks BM (2017). Sensorimotor convergence in circuitry of the motor cortex. *Neuroscientist* **23**, 251–263.

Krings T, Naujokat C & von Keyserlingk DG (1998). Representation of cortical motor function as revealed by stereotactic transcranial magnetic stimulation. *Electroencephalogr Clin Neurophysiol* **109**, 85–93.

Kruglikov I & Rudy B (2008). Perisomatic GABA release and thalamocortical integration onto neocortical excitatory cells are regulated by neuromodulators. *Neuron* **58**, 911–924.

Kunesch E, Knecht S, Schnitzler A, Tyercha C, Schmitz F & Freund HJ (1995). Somatosensory evoked potentials elicited by intraneural microstimulation of afferent nerve fibres. *J Clin Neurophysiol* **12**, 476–487.

Lotti F, Ranieri F, Vadalà G, Zollo L & Di Pino G (2017). Invasive intraneural interfaces: foreign body reaction issues. *Front Neurosci* **11**, 497.

Mackert BM, Sappok T, Grüsser S, Flor H & Curio G (2003). The eloquence of silent cortex: analysis of afferent input to deafferented cortex in arm amputees. *Neuroreport* **14**, 409–412.

Makeig S, Debener S, Onton J & Delorme A (2004). Mining event-related brain dynamics. *Trends Cogn Sci* **8**, 204–210.

Mastinu E, Engels LF, Clemente F, Dione M, Sassu P, Aszmann O, Brånemark R, Håkansson B, Controzzi M, Wessberg J, Cipriani C & Ortiz-Catalan M (2020). Neural feedback strategies to improve grasping coordination in neuromusculoskeletal prostheses. *Sci Rep* **10**, 11793.

Matyas F, Sreenivasan V, Marbach F, Wacongne C, Barsy B, Mateo C, Aronoff R & Petersen CC (2010). Motor control by sensory cortex. *Science* **330**, 1240–1243.

Molier BI, Van Asseldonk EH, Hermens HJ & Jannink MJ (2010). Nature, timing, frequency and type of augmented feedback; does it influence motor relearning of the hemiparetic arm after stroke? A systematic review. *Disabil Rehabil* **32**, 1799–1809.

Nannini N & Horch K (1991). Muscle recruitment with intrafascicular electrodes. *IEEE Trans Biomed Eng* **38**, 769–776.

Navarro X, Krueger TB, Lago N, Micera S, Stieglitz T & Dario P (2005). A critical review of interfaces with the peripheral nervous system for the control of neuroprostheses and hybrid bionic systems. *J Peripher Nerv Syst* **10**, 229–258.

Oddo CM, Raspopovic S, Artoni F, Mazzoni A, Spigler G, Petrini F, Giambattistelli F, Vecchio F, Miraglia F, Zollo L, Di Pino G, Camboni D, Carrozza MC, Guglielmelli E, Rossini PM, Faraguna U & Micera S (2016). Intraneural stimulation elicits discrimination of textural features by artificial fingertip in intact and amputee humans. *Elife* **5**, e09148.

Oddsson LIE, Bisson T, Cohen HS, Jacobs L, Khoshnoodi M, Kung D, Lipsitz LA, Manor B, McCracken P, Rumsey Y, Wrisley DM & Koehler-McNicholas SR (2020). The effects of a wearable sensory prosthesis on gait and balance function after 10 weeks of use in persons with peripheral neuropathy and high fall risk–the walk 2 wellness trial. *Front Aging Neurosci* **12**, 592751.

Ortiz-Catalan M, Hakansson B & Branemark R (2014). An osseointegrated human-machine gateway for long-term sensory feedback and motor control of artificial limbs. *Sci Transl Med* **6**, 257re6.

Ozaki I & Hashimoto I (2011). Exploring the physiology and function of high-frequency oscillations (HFOs) from the somatosensory cortex. *Clin Neurophysiol* **122**, 1908–1923.

Pascual-Leone A, Peris M, Tormos JM, Pascual AP & Catalá MD (1996). Reorganization of human cortical motor output maps following traumatic forearm amputation. *Neuroreport* **7**, 2068–2070.

Pellegrino G, Machado A, von Ellenrieder N, Watanabe S, Hall JA, Lina JM, Kobayashi E & Grova C (2016*a*). Hemodynamic response to interictal epileptiform discharges addressed by personalized EEG-fNIRS recordings. *Front Neurosci* **10**, 102.

Pellegrino G, Hedrich T, Chowdhury R, Hall JA, Lina JM, Dubeau F, Kobayashi E & Grova C (2016*b*). Source localization of the seizure onset zone from ictal EEG/MEG data. *Hum Brain Mapp* **37**, 2528–2546.

Pellegrino G, Hedrich T, Chowdhury RA, Hall JA, Dubeau F, Lina JM, Kobayashi E & Grova C (2018). Clinical yield of magnetoencephalography distributed source imaging in epilepsy: a comparison with equivalent current dipole method. *Hum Brain Mapp* **39**, 218–231.

Peterson NN, Schroeder CE & Arezzo JC (1995). Neural generators of early cortical somatosensory evoked potentials in the awake monkey. *Electroencephalogr Clin Neurophysiol* **96**, 248–260.

Petrini FM, Valle G, Strauss I, Granata G, Di Iorio R, D'Anna E, Čvančara P, Mueller M, Carpaneto J, Clemente F, Controzzi M, Bisoni L, Carboni C, Barbaro M, Iodice F, Andreu D, Hiairrassary A, Divoux JL, Cipriani C, Guiraud D, Raffo L, Fernandez E, Stieglitz T, Raspopovic S, Rossini PM & Micera S (2019). Six-month assessment of a hand prosthesis with intraneural tactile feedback. *Ann Neurol* **85**, 137–154.

Pilurzi G, Ginatempo F, Mercante B, Cattaneo L, Pavesi G, Rothwell JC & Deriu F (2020). Role of cutaneous and proprioceptive inputs in sensorimotor integration and plasticity occurring in the facial primary motor cortex. *J Physiol* **598**, 839–851.

Poppendieck W, Muceli S, Dideriksen J, Rocon E, Pons JL, Farina D & Hoffmann KP (2015). A new generation of double-sided intramuscular electrodes for multi-channel recording and stimulation. *Conf Proc IEEE Eng Med Biol Soc* **2015**, 7135–7138.

Pratt H, Starr A, Amlie RN & Politoske D (1979). Mechanically and electrically evoked somatosensory potentials in normal humans. *Neurology* **29**, 1236–1244.

Raffin E, Pellegrino G, Di Lazzaro V, Thielscher A & Siebner HR (2015). Bringing transcranial mapping into shape: Sulcus-aligned mapping captures motor somatotopy in human primary motor hand area. *Neuroimage* **120**, 164–175.

Raspopovic S, Capogrosso M, Petrini FM, Bonizzato M, Rigosa J, Di Pino G, Carpaneto J, Controzzi M, Boretius T, Fernandez E, Granata G, Oddo CM, Citi L, Ciancio AL, Cipriani C, Carrozza MC, Jensen W, Guglielmelli E, Stieglitz T, Rossini PM & Micera S (2014). Restoring natural sensory feedback in real-time bidirectional hand prostheses. *Sci Transl Med* **6**, 222ra19.

Rathelot JA & Strick PL (2006). Muscle representation in the macaque motor cortex: an anatomical perspective. *Proc Natl Acad Sci U S A* **103**, 8257–8262.

Rathelot JA, Dum RP & Strick PL (2017). Posterior parietal cortex contains a command apparatus for hand movements. *Proc Natl Acad Sci U S A* **114**, 4255–4260.

Robbe D (2018). To move or to sense? Incorporating somatosensory representation into striatal functions. *Curr Opin Neurobiol* **52**, 123–130.

Röricht S, Meyer BU, Niehaus L & Brandt SA (1999). Long-term reorganization of motor cortex outputs after arm amputation. *Neurology* **53**, 106–111.

Rossini PM, Micera S, Benvenuto A, Carpaneto J, Cavallo G, Citi L, Cipriani C, Denaro L, Denaro V, Di Pino G, Ferreri F, Guglielmelli E, Hoffmann KP, Raspopovic S, Rigosa J, Rossini L, Tombini M & Dario P (2010). Double nerve intraneural interface implant on a human amputee for robotic hand control. *Clin Neurophysiol* **121**, 777–783.

Schady WJ, Torebjörk HE & Ochoa JL (1983). Peripheral projections of nerve fibres in the human median nerve. *Brain Res* **277**, 249–261.

Strauss I, Valle G, Artoni F, D'Anna E, Granata G, Di Iorio R, Guiraud D, Stieglitz T, Rossini PM, Raspopovic S, Petrini FM & Micera S (2019). Characterization of multi-channel intraneural stimulation in transradial amputees. *Sci Rep* **9**, 19258.

Tadel F, Baillet S, Mosher JC, Pantazis D & Leahy RM (2011). Brainstorm: a user-friendly application for MEG/EEG analysis. *Comput Intell Neurosci* **2011**, 1.

Tamburin S, Fiaschi A, Andreoli A, Marani S & Zanette G (2005). Sensorimotor integration to cutaneous afferents in humans: the effect of the size of the receptive field. *Exp Brain Res* **167**, 362–369.

Tan DW, Schiefer MA, Keith MW, Anderson JR, Tyler J & Tyler DJ (2014). A neural interface provides long-term stable natural touch perception. *Sci Transl Med* **6**, 257ra138.

Tokimura H, Di Lazzaro V, Tokimura Y, Oliviero A, Profice P, Insola A, Mazzone P, Tonali P & Rothwell JC (2000). Short latency inhibition of human hand motor cortex by somatosensory input from the hand. *J Physiol* **523**, 503–513

Valle G, Mazzoni A, Iberite F, D'Anna E, Strauss I, Granata G, Controzzi M, Clemente F, Rognini G, Cipriani C, Stieglitz T, Petrini FM, Rossini PM & Micera S (2018). Biomimetic intraneural sensory feedback enhances sensation naturalness, tactile sensitivity, and manual dexterity in a bidirectional prosthesis. *Neuron* **100**, 37–45.e7.

Xiang Z, Huguenard JR & Prince DA (1998). Cholinergic switching within neocortical inhibitory networks. *Science* **281**, 985–988.

Zollo L, Di Pino G, Ciancio AL, Ranieri F, Cordella F, Gentile C, Noce E, Romeo RA, Dellacasa-Bellingegni A, Vadalà G, Miccinilli S, Mioli A, Diaz-Balzani L, Bravi M, Hoffmann KP, Schneider A, Denaro L, Davalli A, Gruppioni E, Sacchetti R, Castellano S, Di Lazzaro V, Sterzi S, Denaro V & Guglielmelli E (2019). Restoring tactile sensations via neural interfaces for real-time force-and-slippage closed-loop control of bionic hands. *Sci Robot* **4**, eaau9924.

Additional information

Data availability statement

All data supporting the results presented in this paper are included in the figures and tables. Datasets of scalp somatosensory evoked potentials, compound muscle action potentials and motor evoked potentials are made publicly available in the FigShare repository through the link: https://doi.org/10.6084/m9.figshare.17088857. MRI and EEG data are made available by the authors upon reasonable request and agreement on personal data protection rules.

Competing interests

The authors declare that the research was conducted in the absence of any commercial or financial relationships that could be construed as a potential conflict of interest.

Author contributions

F.R., V.D. and G.D. contributed to the conception and design of the work. Experiments were performed by F.R., A.L.C.,

G.M., E.N., A.I. and L.A.D.B. in the laboratories of Campus Bio-Medico University of Rome. F.R., G.P. and G.D. analysed the data, drafted the manuscript and prepared the figures. All authors contributed to the interpretation of the data and revised the article for intellectual content. All authors approved the final version. All authors agree to be accountable for all aspects of the work. All persons designated as authors qualify for authorship, and all those who qualify for authorship are listed.

Acknowledgement

Open Access Funding provided by Universita degli Studi di Verona within the CRUI-CARE Agreement.

Funding

This work was supported by the Italian National Institute for Insurance against Accidents at Work (INAIL) with PPR2 project 'Control of upper-limb prosthesis with invasive neural interfaces' (CUP: E58C13000990001) and with RGM5 project 'Re-Give Me Five' (CUP: PEN0134) and by the European Research Council (ERC) Starting Grant 2015 RESHAPE 'REstoring the Self with embodiable Hand ProsthesEs' (ERC-2015-STG, project no. 678908).

Keywords

evoked potentials, intraneural double-sided filament electrodes (ds-FILE), short-latency afferent inhibition, somatosensory peripheral stimulation, transcranial magnetic stimulation (TMS)

Supporting information

Additional supporting information can be found online in the Supporting Information section at the end of the HTML view of the article. Supporting information files available:

Peer Review History
Statistical Summary Document